Geometric Calibration of an Over-Constrained CDPR using Partial End-Effector Pose Measurement

Saman Lessanibahri, Hélène Chanal, Chedli Bouzgarrou and Marc Gouttefarde

Abstract This paper presents a geometric calibration method of a spatial over-constrained Cable-Driven Parallel Robot (CDPR) using partial external pose measurement, where only the position of the moving platform is measured by a laser tracker. The CDPR under study is actuated by spiral winch drums. Therefore, this paper presents an adapted model of the winch and its associated identification process. A laser tracker along with actuator encoder data is used for calibration of the model of the CDPR prototype. The proposed calibration method is validated using the measurement data collected via the laser tracker. The validation results show an overall average improvement in position accuracy of the moving platform from 1.1 to 0.47 mm.

1 Introduction

Cable-driven parallel robots (CDPRs) are parallel manipulators that are actuated by cables. CDPRs are well-known for outperforming conventional parallel manipulators in terms of reconfigurability, large workspace-to-footprint ratio, heavy payload capa-bilities, and high acceleration, etc. [1]. Figure 1 shows the CDPR prototype of CABTIVE project at Clermont, which is the subject of geometric calibration in this study.

Using a CDPR for Fused Deposition Modeling (FDM) additive manufacturing of medium-sized pieces requires sub-millimeter accuracy in end-effector positioning. Manufacturing and assembly tolerances introduce geometric errors,

Saman Lessanibahri, Hélène Chanal, Chedli Bouzgarrou. Université Clermont Auvergne, CNRS, Clermont Auvergne INP, Institut Pascal, Clermont-Ferrand, France.
Marc Gouttefarde. LIRMM, Univ Montpellier, CNRS, Montpellier, France.

causing a devia-tion in the geometric model from its nominal behavior. Hence, the calibration and identification of the manipulator geometric parameters, such as pulley positions, winch radii, and Moving Platform (MP) anchor points are fundamental steps to guar-antee its overall positioning performance. Therefore, various geometric calibration methods are detailed in the literature. A comparison between two main calibration methods, namely calibration with external measurements and self-calibration, is pre-sented by Dit Sandretto et al. in [2].

The calibration of geometric parameters is a well-established problem in parallel robotics and several seminal works have established the theoretical foundation for both self-calibration and external calibration methods [3-7]. The selection of calibra-tion poses is an important issue in geometric calibration [8-12]. In this study, the poses were selected randomly while ensuring sufficient variation in the platform posi-tion and orientation. Miermeister et al. in [13] used internal sensors (motors' encod-ers) for the auto-calibration of CDPRs showing a good correspondence between model predictions and experimental measurements. In [14], the kinematic calibration of a triple-level spatial positioner consisting of a CDPR, an active gyro stabilizer and a Stewart platform is studied using 6 Degree-of-Freedom (DoF) laser tracker pose measurement. A planar over-constrained CDPR and its two self-calibration approach-es, i.e., tension-based and jitter-based ones, are presented in [15]. Martin et al. in [16] proposes a cable length measurement correction method based on a direct cable length measurement sensor as a possible application toward auto-calibration of CDPRs.

Unlike the self-calibration approaches described above, exteroceptive calibration us-es measurement systems such as laser trackers. These systems can provide high meas-urement accuracy (typically in the order of tens of micrometers) and can significantly improve the geometric accuracy of CDPRs after calibration. However, they require a clear line of sight and involve higher equipment costs, while self-calibration methods rely only on internal sensors but may suffer from observability issues and generally provide lower measurement accuracy. Hamann et al. in [17] developed an identifica-tion method based on radial basis functions and laser tracker measurements for the geometric parameters of a 3-DoF reconfigurable CDPR. While their approach relies on a data-driven approximation of the geometric error, the method proposed in this paper follows a model-based calibration strategy relying on an explicit geometric model of the CDPR.

This paper makes two primary contributions to the geometric calibration of over-constrained CDPRs. First, it uses partial pose measurements obtained with a laser tracker to determine the 3D position of the MP. Second, the paper models the spiral winch drums employed in the CDPR. Most CDPRs studied in prior works use radial winch drums.

2 CDPR Parameterization and Modeling

This research work aims to develop a CDPR offering high static and dynamic performance needed for 3D printing of medium-sized pieces. The corresponding prototype is driven by 8 cables in an over-constrained configuration and is shown in Fig. 1(right).

2.1 Geometric Model

For the calibration method under study, the geometric model of the CDPR with pulley is considered. Compared to the commonly used simplified model where the cable anchor point is fixed, this model eliminates systematic kinematic errors, and thereby improves the positioning accuracy of the MP [18]. The CDPR geometric model is based on the modeling approach presented in [19], which takes the pulley geometry into account by computing the cable exit point and direction at the pulley. This approach is based on an already-known modeling method.

Figure 1 (left) shows the schematic representation of the main geometric parameters used in the CDPR. The MP reference point C is defined as the origin of the MP frame $\mathcal{R}_{MP}$ and its position in the base frame $\mathcal{R}_0$ is denoted by ${}^0\boldsymbol{c}_j$. The loop-closure relation of the CDPR for cable i at pose j is given in Eq. (1). The vector ${}^{e_i}\boldsymbol{l}_{j,i}$ denotes the vector from the MP anchor point B_i to pulley exit-point A_i, expressed in i-th pulley frame $\mathcal{R}_{e_i}$. The active cable length is then calculated as $\left\| {}^{e_i}\boldsymbol{l}_{j,i} \right\|_2$. The rotation matrix from $\mathcal{R}_{MP_j}$ to the base frame $\mathcal{R}_0$ is given by ${}^0\boldsymbol{R}_{MP_j}$, while the rotation matrix from $\mathcal{R}_0$ to $\mathcal{R}_{e_i}$ is ${}^{ei}\boldsymbol{R}_{0_j}$. The vector ${}^{MP}\boldsymbol{b}_i$ represents the coordinates of B_i expressed in $\mathcal{R}_{MP}$. ${}^{e_i}\boldsymbol{n}_{j,i}$ denotes the cable vector corresponding to the portion of cable wound on the pulley between A_i to P_i. It is a function of the pulley radius $r_{p,\,i}$ and pulley orientation. Finally, the Cartesian coordinates vector of P_i and C_j in $\mathcal{R}_0$ are defined by ${}^0\boldsymbol{p}_i$ and ${}^0\boldsymbol{c}_j$, respectively.

$$ {}^{e_i}\boldsymbol{l}_{j,i} + {}^{e_i}\boldsymbol{n}_{j,i} = {}^{e_i}\boldsymbol{R}_{0_j} \left({}^0\boldsymbol{p}_i - {}^0\boldsymbol{c}_j - {}^0\boldsymbol{R}_{MP_j}{}^{MP}\boldsymbol{b}_i \right), \qquad i = 1, \dots, 8\ , \qquad j = 1, \dots, J \quad (1) $$

Building on this geometric description, the next subsection presents the winch model, which relates the spiral winch actuation to the amount of cable effectively wound/unwound, and hence to the active cable length introduced in the loop-closure equations.

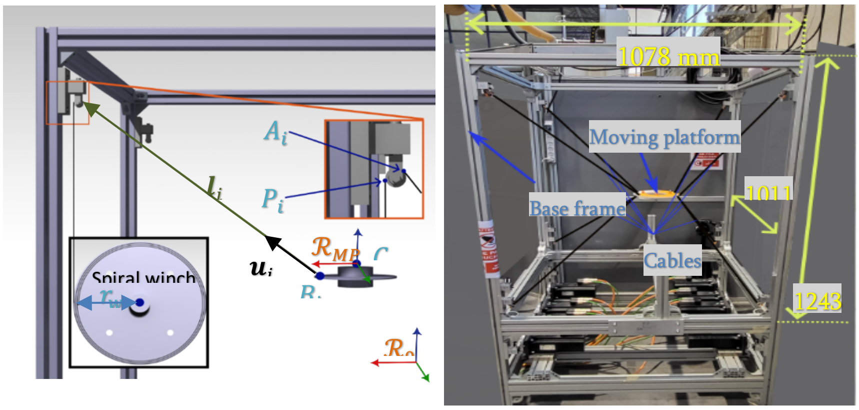

Fig. 1. (Left) Schematic representation of the cable routing and spiral winch drum geometry used in the geometric model – (Right) CABTIVE prototype for FDM 3D printing.

2.2 Spiral Winch Model

Two main drum geometries are commonly used in CDPR winches: radial and spiral. Spiral ones (Fig. 1) are less studied and employed in CDPRs. Unlike radial winch design, the spiral winch drum relies on the variation of the winding radius as the cable winds on the previous layer, resulting in a compact design but a varying transmission ratio between the motor angle and cable length. The spiral winch model is formulated as follows:

$$l_{p,i} = sign(\theta_{p,i}) \cdot \left[\underbrace{\left(|\theta_{p,i}| - 2\pi n_{p,i}\right).\left(r_{w,i} + n_{p,i}\, d_c\right)}_{l_{partial}} + \underbrace{2\pi \sum_{k=0}^{n_{p,i}-1} \left(r_{w,i} + k d_c\right)}_{l_{full}} \right] \quad (2)$$

where i denotes the cable number, $p \in \{0, j\}$ denotes the pose index ($p = 0$ corresponds to the home pose and $p = j\ to$ pose j), $\theta_{p,i}$ is the angular displacement of motor i at pose p where $\theta_{p,i} = 0$ corresponds to the configuration where the cable of winch i just begins to wind around the drum, and $sign(\theta_{p,i})$ indicates whether cable i is being wound (-) or unwound (+). The variable $l_{p,i}$ represents the length of cable i at pose p, while $n_{p,i}$ denotes the number of complete revolutions of cable i around the winch drum at pose p. The parameter $r_{w,i}$ is the initial winch radius (first cable layer), and d_c is the cable diameter. In Eq. (2), l_{full} represents the cable length corresponding to the fully wound layers of the drum, while $l_{partial}$ corresponds to the cable length wound during the remaining angular displacement on the current layer. The cable is routed from the winch to the MP through a pair of pulleys: the first is fixed to the base frame, while the second is a swiveling pulley that redirects the cable toward the MP, ensuring that the cable configuration remains fixed between the winch exit point and point P_i. Finally, the difference in the wound/unwound cable length on the winches with respect to the home pose ($p = 0$) is the active cable length:

$$\left\| {}^{e_i}\boldsymbol{l}_{j,i} \right\|_2 = \Delta l_{j,i} = l_{j,i} - l_{0,i} \tag{3}$$

This spiral winch drum model enables the conversion of motor encoder measurements into accurate cable length variations. This transmission model therefore allows precise cable length estimation, providing the information required for the geometric parameter calibration process.

2.3 Geometric Parameters

This subsection presents the complete set of geometric parameters that are considered for geometric calibration. A total of 65 parameters are listed in Table 1.

Table 1. Geometric calibration parameters

Parameter	symbol		Total parameters
Pully points	${}^{0}\boldsymbol{p}_i = [p_{i,x} \quad p_{i,y} \quad p_{i,z}]^T,$	$i = 1, \dots, 8$	24
Anchor points	${}^{MP}\boldsymbol{b}_i = [b_{i,x} \quad b_{i,y} \quad b_{i,z}]^T,$	$i = 1, \dots, 8$	24
Winch drum radii	$r_{w,\,i}$,	$i = 1, \dots, 8$	8
Pulley radii	$r_{p,\,i}$,	$i = 1, \dots, 8$	8
Cable diameter	d_c		1

3 Proposed Calibration Method

The proposed calibration of the geometrical parameters of the CDPR is formulated as a hierarchical optimization problem. The overall process consists of an outer optimization loop (the main optimizer) and one nested optimizer that solves the direct kinematics, i.e., the pose of the MP for eight given cable lengths. The calibration procedure is performed offline using recorded measurement data from the laser tracker and actuator encoders. The complete set of the all parameters listed in Tab. 1 is considered for the calibration as follows:

$$\boldsymbol{\xi} = \left[{}^{0}\boldsymbol{p}_1{}^T, \dots, {}^{0}\boldsymbol{p}_8{}^T, {}^{MP}\boldsymbol{b}_1{}^T, \dots, {}^{MP}\boldsymbol{b}_8{}^T, r_{w,1}, \dots, r_{w,8},, r_{p,1}, \dots, r_{p,8}, d_c\right]^T \in \mathbb{R}^{65} \quad (4)$$

It should be noted that, the pulley radii $r_{p,i}$ are included in the geometric modeling of the CDPR and follow the formulation described in [19]. The main identification optimizer aims to find the optimal parameters set $\boldsymbol{\xi}_{opt}$ that minimize the total position error of the MP across all measurement configurations ($error$) as follows:

1- Initialization: The parameters are initialized as $\boldsymbol{\xi} = \boldsymbol{\xi}_0$ with their respective lower and upper bounds, $\boldsymbol{\xi}_{lb}$ and $\boldsymbol{\xi}_{ub}$. The initial values are selected based on the nominal dimensions obtained from the CAD model and measurement data while the bounds are defined to allow reasonable deviations to account for possible assembly and measurement uncertainties.

2- Cost function evaluation: For the current $\boldsymbol{\xi}$, the calibration procedure involves an outer optimization loop and a nested nonlinear least-squares optimization used to solve the Direct Geometric Model (DGM).

- *Inverse Geometric Model (IGM)*: It calculates the cable lengths for measured geometric parameters, including the position ${}^{0}\boldsymbol{c}_0$ and orientation ${}^{0}\boldsymbol{R}_{MP}$ of the MP. In the case of $p = 0$ (home pose), the second norm of the cable length vector $||\boldsymbol{l}_0||_2$ is calculated by applying Eq. (1) to the home pose configuration, where $\boldsymbol{l}_0$ represents the vector of cable lengths corresponding to this reference pose. The home pose of the MP, including both its position and orientation, is measured by the laser tracker.

- *DGM*: For each j, the pose of the MP, including both position and orientation, is estimated from the cable length equations. Since the number of cable equations exceeds the six unknown pose variables, the system is solved in a nonlinear least-squares sense by minimizing the residual between the cable lengths obtained from the winch model and those predicted by the geometric model:

$$\min_{\boldsymbol{x}_j} \sum_{i=1}^{8} (l_{m,j,i} - l_i(\boldsymbol{x}_j, \boldsymbol{\xi}))^2 \tag{5}$$

where $\boldsymbol{x}_j$ denotes the pose of the MP, $l_{m,j,i}$ is the i-th cable length obtained from the winch model and $l_i(\boldsymbol{x}_j, \boldsymbol{\xi})$ is the cable length predicted by the DGM.

- ***Residual computation***: The predicted MP position $\boldsymbol{c}_{pred,j}$, extracted from the estimated pose $\boldsymbol{x}_j$, is compared with the position measured by the laser tracker $\boldsymbol{c}_{mes,j}$.
- *Main calibration cost*: The current parameter vector $\boldsymbol{\xi}$ is calculated as one minimizing the total sum of the Euclidean norms of position residuals over all recorded measurement poses:

$$\min_{\boldsymbol{\xi}} \sum_{j=0}^{J} \left\| \boldsymbol{c}_{pred,j}(\boldsymbol{\xi}) - \boldsymbol{c}_{mes,j} \right\|_2 \tag{6}$$

- *Dataset iteration*: Set $j \leftarrow j + 1$ and repeat the winch model, DGM, and residual computation steps for the next dataset.

3- Convergence check: If the convergence criteria of the outer optimizer are satisfied, the current parameter vector is taken as the optimal solution $\boldsymbol{\xi}_{opt}$. The solver stops when the parameter updates and the residual norm, or both fall below a pre-defined tolerance, or when the first-order optimality is satisfied. Maximum iteration and function-evaluation limits are also enforced.

The calibration procedure is carried out under the following hypotheses. All measurements are performed under static conditions. The cables are made of stainless steel and are assumed to remain perfectly taut, neglecting sagging and elasticity effects. A small pretension is applied during the calibration experiments to ensure that all cables remain taut, and therefore cable slackness is not considered in the modeling. The CDPR base frame is considered rigid (no deformation). The base frame reference is obtained by measuring the center of the base frame with the laser tracker, and an additional measured point along the x-direction of the frame defines the x-axis orientation. The z-axis is aligned with the gravity vector provided by the laser tracker. The anchor points on the MP, B_i, are perfectly fixed to the MP. The pose of the MP in its home position is fixed and repeatable during the whole measurement.

Most of the initial geometric parameters of the prototype can be measured by conventional measurement tools. However, some can hardly be measured directly and are therefore estimated from the CAD model. The former includes the fixed pulley points P_i, the pulley radii $r_{p,i}$, the winch radii $r_{w,i}$ and the cable diameter d_c. The latter includes the initial cable lengths $l_{0,i}$ and the position vector of the MP anchor points expressed in the MP frame, ${}^{MP}\boldsymbol{b}_i$. Table 2 gives the measured coordinates of the cable exit points corresponding to the pully fixed points P_i and Table 3 shows the coordinates of the cable anchor points to the MP.

Table 2. Cartesian coordinates of the pulley fixed points (mm) in the base frame

Coordinates	${}^0\boldsymbol{p}_1$	${}^0\boldsymbol{p}_2$	${}^0\boldsymbol{p}_3$	${}^0\boldsymbol{p}_4$	${}^0\boldsymbol{p}_5$	${}^0\boldsymbol{p}_6$	${}^0\boldsymbol{p}_7$	${}^0\boldsymbol{p}_8$
x	861.1	-140	-141.4	860.4	860.7	-139.1	-139.1	859.8
y	1058.3	1058.7	56.2	57.7	1061.3	1060.5	60.3	59.7
Z	1097.1	1096.2	1091.4	1092.8	44	43.1	36.8	41.6

Table 3. Cartesian coordinates of the MP cable anchor points (mm) in the platform frame.

Coordinates	${}^{MP}\boldsymbol{b}_1$	${}^{MP}\boldsymbol{b}_2$	${}^{MP}\boldsymbol{b}_3$	${}^{MP}\boldsymbol{b}_4$	${}^{MP}\boldsymbol{b}_5$	${}^{MP}\boldsymbol{b}_6$	${}^{MP}\boldsymbol{b}_7$	${}^{MP}\boldsymbol{b}_8$
x	49.9	-49.9	-49.9	49.9	27.3	-27.3	-27.3	27.3
y	86.6	86.6	−86.6	-86.6	96.1	96.1	-96.1	-96.1
z	-73	-73	-73	-73	-73	-73	-73	-73

The other geometric parameters are $r_{p,i} =$ 8.6 mm, $r_{w,i} = 60$, mm for $i = 1, \dots, 8$ and $d_c =$ 0.48 mm.

4 Calibration Results and Validation

This section focuses on the validation of the proposed calibration method using laser tracker measurements. The initial (nominal) geometric parameters used to start the optimization are first reported, followed by the estimated optimal parameter values obtained after calibration. Finally, the resulting improvements are quantified by comparing the MP position error before and after calibration. Ninety poses were randomly selected to ensure a broad variety of translations and orientations of the MP. The laser tracker measured only the position of the MP, while its orientation was estimated through the geometric model during the calibration process. For the validation measurement set, ten complete poses were captured.

The calibration parameters are estimated in MATLAB by solving a nonlinear least-squares problem using MATLAB function `lsqnonlin`. Bound constraints are imposed to enforce physically meaningful parameter ranges, as given in Tab.4. Central finite differences are used for Jacobian approximation. The solver stops when the step tolerance, function tolerance, or first-order-optimality reaches 10^{-6}, 10^{-20}, and 10^{-27}, respectively. The maximum number of iteration and function evaluation is set to 250 and 10^{13}, respectively.

Table 4. Parameters bounds used in a nonlinear least-squares optimization

Parameter	Bounds
Exit points (mm)	${}^{0}p_{p,i\,init} - 10 \leq {}^{0}p_{p,i} \leq {}^{0}p_{p,i\,init} + 10\,, \quad i = 1, \ldots, 8\,,\ p = x, y, z$
Anchor points (mm)	${}^{MP}b_{p,i\,init} - 10 \leq {}^{MP}b_{p,i} \leq {}^{MP}b_{p,i\,init} + 10\,, \quad i = 1, \ldots, 8\,,\ p = x, y, z$
Winch radius (mm)	$59 \leq r_{w,i} \leq 61\,, \quad i = 1, \ldots, 8$
Pulley radius (deg)	$7.7 \leq r_{p,i} \leq 9.3\,, \quad i = 1, \ldots, 8$
Cable diameter(mm)	$0.42 \leq d_c \leq 0.58$

Finally, the optimal cable diameter is computed as $d_{c,opt} = 0.422$ mm. The other optimal geometric parameter values are given in Tabs. 5, 6 and 7.

Table 5. Optimal Cartesian coordinates of pulley fixed points (mm)

Coordinates	${}^{0}\boldsymbol{p}_{1,opt}$	${}^{0}\boldsymbol{p}_{2,opt}$	${}^{0}\boldsymbol{p}_{3,opt}$	${}^{0}\boldsymbol{p}_{4,opt}$	${}^{0}\boldsymbol{p}_{5,opt}$	${}^{0}\boldsymbol{p}_{6,opt}$	${}^{0}\boldsymbol{p}_{7,opt}$	${}^{0}\boldsymbol{p}_{8,opt}$
x	859.4	-143.3	-131.5	850.6	861.2	-130.2	-139.8	860.4
y	1067.8	1063.4	55.9	58.7	1071.2	1068.8	53.3	56.8
z	1106.7	1105.8	1101.2	1102.5	53.8	51	46.8	51.5

Table 6. Optimal Cartesian coordinates of the cable anchor point to the MP (mm)

Coordinates	${}^{MP}\boldsymbol{b}_{1,opt}$	${}^{MP}\boldsymbol{b}_{2,opt}$	${}^{MP}\boldsymbol{b}_{3,opt}$	${}^{MP}\boldsymbol{b}_{4,opt}$	${}^{MP}\boldsymbol{b}_{5,opt}$	${}^{MP}\boldsymbol{b}_{6,opt}$	${}^{MP}\boldsymbol{b}_{7,opt}$	${}^{MP}\boldsymbol{b}_{8,opt}$
x	43.4	-40	-54.6	55	32.4	-21.6	-30.9	32.6
y	92.4	95	-93.4	-90.5	106	102.4	-99.6	-106
z	-63.3	-63.1	-71.3	-66.4	-65.6	-62.9	-62.6	-63.7

Table 7. Optimal pulley and winch radii (mm)

i (Cable index)	1	2	3	4	5	6	7	8
$r_{p,opt}$	8	7.9	7.9	7.8	7.7	8.4	8	8.5
$r_{w,opt}$	59	59	60.2	59	60.4	60.1	60.5	60.1

The position measurement of the MP and the corresponding motor encoder data acquisition for a given pose take a few minutes. The calibration optimization calculations require approximately 57 minutes when executed on a laptop equipped with an Intel Core Ultra 9 processor.

The optimized parameters yield $error(\boldsymbol{\xi}_{\text{opt}}) = 0.38$ mm between the model and the measurement, compared with $error(\boldsymbol{\xi}_{\text{nom}}) = 1.6$ mm for the nominal parameters, corresponding to a 76% error reduction. To assess the predictive capability of the calibrated model, an independent validation set of 10 additional poses not used during the calibration was considered. For these poses, the nominal model yields a position error of **1.1 mm**, whereas the calibrated model results in a position error of **0.47 mm** and an orientation error of **0.5°**.

5 Conclusion

This paper introduced the geometric parameter calibration of an over-constrained CDPR prototype intended for FDM 3D printing. The geometric model of the proto-type including that of its spiral winches has been presented. A laser tracker has been used as an exteroceptive sensor to measure the position of the CDPR moving plat-form. The optimization of geometric parameters results in the reduction of the average position error of the moving platform from 1.1 mm to 0.47 mm without considering the elasticity of the cables. Future works include the auto-calibration of the prototype using the laser tracker sensor as part of the 3D printing process. The elasticity of the cables will be also included in the modeling to enhance the precision of the 3D print-er CDPR.

Acknowledgments This research was supported by ANR CABTIVE, project number ANR-22-CE10-0008. The authors also acknowledge the project FEDER RobIndus for providing access to the laser tracker sensor. OpenAI tools were used for language editing and improvement of the manuscript.

References

1. Gouttefarde, M., Bruckmann, T., & Pott, A. (Eds.). (2021). Cable-Driven Parallel Robots: Proceedings of the 5th International Conference on Cable-Driven Parallel Robots. Springer Nature.
2. Dit Sandretto, J. A., Daney, D., & Gouttefarde, M. (2013, January). Calibration of a fully-constrained parallel cable-driven robot. In Romansy 19–Robot Design, Dynamics and Control: Proceedings of the 19th CISM-Iftomm Symposium (pp. 77-84). Vienna: Springer Vienna.
3. Everett, L. J. (1989). Forward calibration of closed-loop jointed manipulators. The International journal of robotics research, 8(4), 85-91.
4. Innocenti, C. (1995, September). Algorithms for kinematic calibration of fully-parallel manipulators. In Computational Kinematics' 95: Proceedings of the Second Workshop on Computational Kinematics, held in Sophia Antipolis, France, September 4–6, 1995 (pp. 241-250). Dordrecht: Springer Netherlands.

5. Masory, O., Wang, J., & Zhuang, H. (1996). Kinematic modeling and calibration of a Stewart platform. Advanced Robotics, 11(5), 519-539.
6. Wampler, C. W., Hollerbach, J. M., & Arai, T. (2002). An implicit loop method for kinematic calibration and its application to closed-chain mechanisms. IEEE Transactions on robotics and automation, 11(5), 710-724.
7. Tadokoro, S., Verhoeven, R., Hiller, M., & Takamori, T. (1999, October). A portable parallel manipulator for search and rescue at large-scale urban earthquakes and an identification algorithm for the installation in unstructured environments. In Proceedings 1999 IEEE/RSJ International Conference on Intelligent Robots and Systems. Human and Environment Friendly Robots with High Intelligence and Emotional Quotients (Cat. No. 99CH36289) (Vol. 2, pp. 1222-1227). IEEE.
8. Zoffoli, F., Idà, E., & Carricato, M. (2025). A comparative analysis of initial-pose self-calibration algorithms for underactuated cable-driven parallel robots. Robotica, 1-17.
9. Sandretto, J. A. D., Trombettoni, G., Daney, D., & Chabert, G. (2013, October). Certified calibration of a cable-driven robot using interval contractor programming. In Computational Kinematics: Proceedings of the 6th International Workshop on Computational Kinematics (CK2013) (pp. 209-217). Dordrecht: Springer Netherlands.